Proceedings of the 2011 International Mechanical Engineering Congress and Exposition
ASME/IMECE2011
November 11-17, 2011, Denver, Colorado, USA

IMECE 2011-65255

AERODYNAMIC INFLUENCE OF ENDWALL FENCES LOCATED IN THE VICINITY OF THE LEADING EDGE-ENDWALL JUNCTION OF NOZZLE GUIDE VANES

Zeki Ozgur Gokce[1]
Turbomachinery Aero-Heat Transfer Laboratory
Department of Aerospace Engineering
The Pennsylvania State University
University Park, Pennsylvania 16802
Email: zog100@psu.edu

Cengiz Camci[2]
Turbomachinery Aero-Heat Transfer Laboratory
Department of Aerospace Engineering
The Pennsylvania State University
University Park, Pennsylvania 16802
Email: cxc11@psu.edu

ABSTRACT

Secondary flow characteristics like horseshoe vortices and related total pressure losses decrease turbine efficiency. Computerized simulations of potentially favorable modifications in turbine systems could provide a fast, numerical and inexpensive method of evaluating their effects on flow properties: This paper consists of a comparative numerical study of the flow characteristics of a domain containing a vertical cylinder subjected to cross flow and upstream endwall modifications. Analyzing the flow around a turbine nozzle guide vane (NGV) could be simplified by modeling it as a vertical cylinder with a diameter proportional to the leading edge diameter of the blade, and adding upstream endwall fences of varying dimensions and alignments could attenuate the development of a horseshoe vortex. A commercial computational fluid dynamics (CFD) software package, Fluent, was used for the numerical analysis. To validate the modeling strategy, experimental data previously reported in the literature for conventional cylinders in cross flow were compared to the current predictions. A grid independence study was also performed. The lateral distance between the two legs of the horseshoe vortex downstream of the cylinder was decreased by 7% to 14%. All fence types effectively changed the location of the main horseshoe vortex roll-up. The height of the fence was more influential than the length of the fence in modifying flow characteristics. The existence of the fences slightly increased the mass-averaged total pressure loss far downstream of the cylinder; however, beneficial near-fence flow characteristics were observed in all cases. Also, it was noted that an endwall fence could possibly result in decreased interaction between the horseshoe vortices created by consecutive blades in a row of NGV blades, which would be expected to result in improved flow conditions within actual turbine passages.

INTRODUCTION

The gas turbine is an integral part and a crucial determinant of modern engines. Gas turbine efficiency is related to many factors including secondary flow characteristics, particularly the viscous loss associated with horseshoe vortex formation around turbine blades such as nozzle guide vanes (NGVs) [1]. NGVs receive hot air from combustor exits [2]. Since horseshoe vortices bring in parts of the hot air mentioned, the cooling ability of turbines could be improved if the exact locations of vortex formation were known. Improved turbine cooling, in turn, would enable an increase in the operational total temperature of the turbine inlet and thereby augment engine efficiency [2], [3]. Another adverse effect of horseshoe vortices on turbine efficiency is the total pressure loss accompanying their occurrence [4]. Thus, understanding the properties of flow within turbines in general, and the generation of horseshoe vortices in particular and devising methods to attenuate the latter are required to design better turbines with increased efficiency.

As its name implies, the horseshoe vortex has a horseshoe-like look when viewed from above, i.e. when it is looked at from a perspective directly facing the turbine endwall [5]. Its development is attributed to the momentum deficit generated within the endwall boundary layer and its strength decreases the total pressure within its vicinity [4]. Horseshoe vortices are in general convected into high Mach number regions of turbine passages causing a significant amount of total pressure loss.

One of the most common ways of defining a horseshoe vortex is to describe the separation characteristics relevant to its development [6], [7]. The flow traversing the region over a wall experiences an inevitable separation due to its boundary layer, which occurs at a wall saddle point [6]. The stagnating flow near the saddle point rolls up into a vortex system and creates the horseshoe vortex which is a mixture of the main flow and the boundary layer material [6]. The flow within the boundary layer

[1] Graduate Research Assistant, Ph.D Candidate
[2] Professor of Aerospace Engineering

has relatively lower momentum compared to the free-stream flow outside the boundary layer. In addition, after a certain point, the fluid cannot overcome the adverse pressure gradient generated by the bluff body situated farther downstream [7]. The combination of these two physical facts leads to the formation of a roll-up in the streamwise plane of symmetry, which in turn continues downstream in the shape of a horseshoe.

The generation of horseshoe vortices around turbine blades could possibly be decreased by changing the flow environment. However, a thorough investigation of the behavior of the horseshoe vortex around an actual NGV blade would mandate numerous time consuming and costly experiments. In contrast, analyzing computerized simulations of modifications in a simplified model of a turbine blade or multiple blades would provide a fast, numerical and inexpensive method of evaluating the effects of such modifications on flow attributes. Such analysis could facilitate the design of better turbines by selecting the modifications most worthy of further study under actual experimental conditions and thus create savings in resources. This contention was the underlying idea of this work, which, to our knowledge, is the first comparative numerical study of flow characteristics around a system consisting of a vertical cylinder subjected to cross flow and upstream endwall fences.

Inspired with the idea of examining the crucial aspects of horseshoe vortex formation around a NGV blade with a simplified yet sufficiently accurate model, the vertical cylinder was chosen as its best virtual equivalent. Modeling the leading edge of the NGV blade as a cylinder was considered appropriate since the NGV leading edge diameter dominates the size of the three-dimensional separation over the endwall [5], thereby dictating the main shape and strength of the horseshoe vortex.

Flow characteristics associated with horseshoe vortex formation and its effects have been examined in a number of experimental studies [5-11]. The temporal dynamics of the horseshoe vortex and the resulting heat transfer around a symmetric airfoil shaped vertical body were investigated by Praisner and Smith [8], [9]. Another experimental work regarding flow over a symmetric airfoil was conducted using a Particle Image Velocimetry (PIV) technique by Hada et al. [10]; they concluded that the leading edge diameter has an important influence on the heat transfer near the endwall-leading edge junction and reached an empirical relation where they validated their experimental results with a computational model. Eckerle's PhD thesis study [7] consisted of a detailed investigation of horseshoe vortex development around a cylinder in cross flow and revealed the formation of a single, main horseshoe vortex in the plane of symmetry. He claimed that the Reynolds number used was influential in determining whether multiple vortices would form or not, since his data did not agree with some of the previous work done for very similar configurations, a situation also reported by Visbal [12]. Eckerle and Langston [6] conducted a thorough experimental analysis of the horseshoe vortex formation phenomenon around a vertical cylinder in cross flow. Eckerle and Awad [5] took this experimental study one step further and correlated the formation of the horseshoe vortex to the Reynolds number based on the diameter of the cylinder. Goldstein & Karni [11] contributed to the existing relevant experimental aero-heat transfer data by reporting the effect of mass transfer on the flow around a cylinder in cross flow. To our knowledge, Kang et al. [13] were the first to report the effects of applying an upstream cavity to modify the formation of the horseshoe vortex. The idea of placing endwall fences within turbine passages and in turbines in general to reduce losses has been suggested by some researchers [14-16]. The experimental data obtained prior to the current study indicates that applying changes to the endwall platform at locations where crucial aerodynamic events occur could help reduce losses in turbomachinery flows.

The recent availability of advanced computerized methods, such as multiple computers operating as a cluster, has created the opportunity to study flow domains with differing envisaged modifications. Our research group is currently working on endwall shape modifications to reduce losses in a NGV row located just upstream of a large scale turbine rotor, by combining extensive numerical simulations and gas turbine experiments conducted at the Turbomachinery Aero-Heat Transfer Laboratory of the Pennsylvania State University [17].

The current study is related to the described studies of Turgut [17], because it models certain aspects of the NGV blades used therein. Specifically, the diameter of the model cylinder is equal to twice the leading edge diameter of, and its height is equal to one-sixth of the span of, the NGV blade used by Turgut [17]. These measures were chosen to create a valid model of the NGV blade currently being evaluated in our research laboratory. In order to preserve the ability to compare the two studies, the computations in this study were all carried out at a Reynolds number equal to the Reynolds number calculated based on the leading edge diameter used by Turgut [17]. This was achieved by reducing the inlet velocity profile values used by Turgut [17] by 50%.

To summarize, this study investigated horseshoe vortex formation around a cylinder modeled to simulate a turbine NGV blade, as well as applying various modifications to the endwall shape within the vortex region with the goal of reducing losses without impairing main flow characteristics.

We found that placing a non-oblique or oblique endwall fence upstream of the cylinder decreased the lateral distance between the two legs of the horseshoe vortex downstream of the cylinder by 7% and 14%, respectively, pointing to a decrease in the size of the cylinder wake. All fence types effectively changed the location of the main horseshoe vortex roll-up. We observed that the height of the fence was more influential than its length in modifying flow characteristics, such as the change in the location of the initial vortical roll-up in the streamwise plane of symmetry and the decrease in the wake size. The oblique fence provided an additional benefit in that it did not create secondary vortices in front of or behind it. Endwall fences were associated with an increase in mass-averaged total pressure loss far downstream of the cylinder, but this was offset by an improvement of mass-averaged total

pressure levels near the fence. These findings indicate that the presence of an endwall fence could result in decreased interaction between the horseshoe vortices created by consecutive blades in a row of NGV blades, which in turn could result in improved flow conditions within turbine passages.

The results of this study are of practical relevance because they reveal a method that could potentially decrease horseshoe vortex-related efficiency losses within turbines. Our findings could have important implications for turbomachinery systems and aerospace vehicles. Furthermore, horseshoe vortices are an important issue not only in aerospace engineering, but in other scientific fields as well, such as civil and environmental engineering. For instance, horseshoe vortices forming around cylindrical objects embedded in fluids, such as bridge piers subjected to flowing water, affect the sediment gathering aspects of the relevant fluid and endanger long term performance of the objects in mention [18]. The relevance of our findings may therefore not be limited to aerospace engineering.

We conclude that the effect of adding upstream endwall fences on the flow characteristics of turbines is worthy of further computational as well as experimental research and we are presently realizing such studies [19]. We present our work with the hope of attracting the interest of other research groups to this potentially beneficial method of improving turbine flow characteristics and efficiency.

NOMENCLATURE

Re_D = Reynolds number based on the cylinder diameter = $\frac{\rho U_\infty D}{\mu}$

ρ = Density (kg/m^3)

μ = Viscosity (kg/m.s)

$U_\infty = U_{Inlet}$ = Freestream velocity in the streamwise direction (m/s)

x = Streamwise direction

y = Lateral direction

z = Vertical direction

P_S = Static pressure (Pa)

P_0 = Total pressure (Pa)

$C_{P_S} = \frac{P_{S_{Cylinder}} - P_{S_{Inlet}}}{\frac{1}{2}\rho {U_{Inlet}}^2}$ = Static pressure coefficient

$C_P = \frac{(P_0)_{YZ\ plane} - (P_0)_{Inlet}}{\frac{1}{2}\rho (U_{Inlet})^2}$ = Mass averaged total pressure based C_p within complete y-z planes

$C_P = \frac{(P_0)_{2\ mm\ Strip} - (P_0)_{2\ mm\ Inlet\ Strip}}{\frac{1}{2}\rho (U_{2\ mm\ Inlet\ Strip})^2}$ = Mass averaged total pressure based C_p within complete 2 mm high y-z strips

D = Cylinder diameter (m)

NUMERICAL METHOD

In the present study, the numerical modeling of the flow around the vertical cylinder and the various arrangements of fences were conducted with a commercially available software (FLUENT version 6.3, developed by ANSYS). The meshing of the computational domain was performed with another software (GAMBIT), developed by the same company. The accuracy of results obtained by combining these two software programs was demonstrated by relevant validation studies.

The computational domain consisted of a vertical cylinder of 12 mm diameter and 18 mm height placed in a rectangular field. The domain extended one axial chord length upstream of the cylinder center and two axial chord lengths downstream. The axial chord length chosen was the mid-span axial chord length of the NGV blade used by Turgut [17], Kavurmacioglu et al. [20,21] and Rao et al. [22] and equaled 112.3 mm. The width of the domain was 42 mm and 3.5 times the cylinder diameter. The height of the domain was 18 mm and equal to the cylinder height. The length and width dimensions of the domain were selected large enough to ensure that all flow phenomena could be accurately modeled and captured. Figures 1 and 2 demonstrate the main geometrical properties of the computational domain:

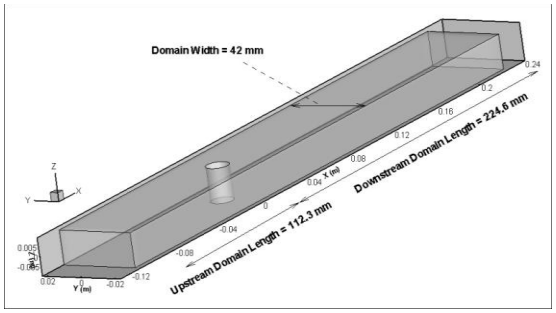

Figure 1. The dimensions of the baseline computational domain

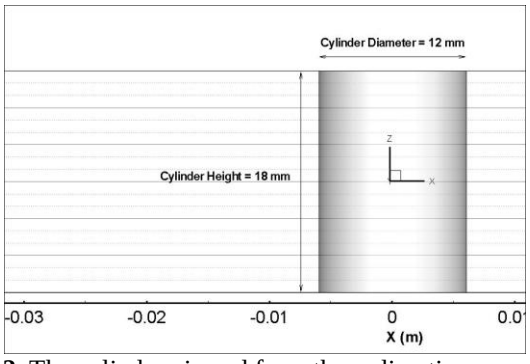

Figure 2. The cylinder viewed from the y-direction

Structured meshes were preferred in this study since they are superior to unstructured simple grids with their higher ability of capturing flow parameter gradients in even the smallest of regions. During mesh design, close attention was given to locations crucial to flow behavior, including the junction of the cylinder and the hub endwall, the junction of the fence and the hub endwall as well as the first 3 millimeters above the hub endwall. Figures 3 and 4 demonstrate certain portions of the mesh:

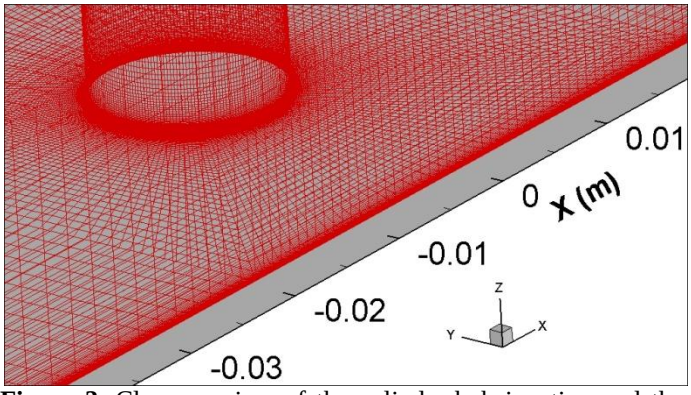

Figure 3. Close-up view of the cylinder-hub junction and the boundary layer region

The baseline case (Case 1) consisted of a cylinder only, with no fence installed. The densest part of the mesh domain of the baseline case was the region surrounding the cylinder, to enable capturing even subtle effects close to it. The cylinder-endwall junction and the boundary layer region contained a particularly concentrated mesh structure. The size of the interval between consecutive nodes along the longitudinal edges decreased from the domain inlet towards the cylinder region. Edge mesh lengths gradually increased from the hub to the top of the domain, to reflect the uniformity of flow at locations outside the boundary layer and sufficiently far from the cylinder. These mesh structure features were adopted to simulate the real time properties of cylinders subjected to cross flow as well as to prevent loss of computational time during analysis.

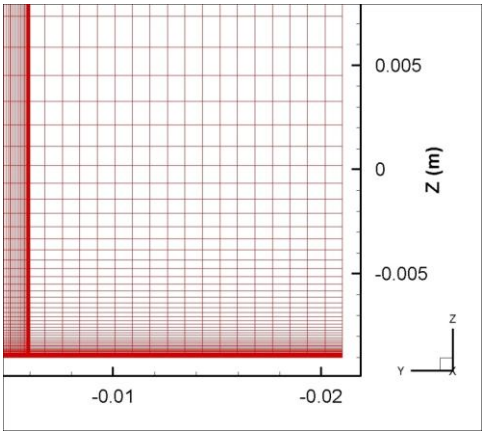

Figure 4. A look at the mesh in the y-z plane

The meshes of the cases with a fence were very similar to the baseline case, except for the quadrant just upstream of the cylinder where the fence was placed. The addition of a fence required dense spacing of nodes on and near itself. The quadrant containing the fence had to be split into smaller volumes of various sizes depending on the geometry of the endwall shape change.

After many preliminary trials with different fences, three fence configurations that appeared most likely to attenuate horseshoe vortex formation were chosen for intensive study: a non-oblique fence 1 mm high, 1 mm deep and 4 mm long (Case 2), a 1 mm high, 1 mm deep and 4 mm long fence with oblique lateral sides (Case 3) and another non-oblique fence 1 mm high, 1 mm deep and 2 mm long (Case 4).

The *height* of the fence refers to its length in the z-direction, its *depth* refers to its length in the x-direction (streamwise direction), and its *length* refers to its length in the y-direction.

The center of the main vortex, i.e. the approximate location of the center of the main roll-up in the plane of symmetry for the baseline case, was chosen as the point where the center of the two-dimensional cross sections of the fences were placed for cases containing fences. The aim of selecting this particular location was its high potential to affect the shape and/or the strength and/or effects of the main horseshoe vortex without affecting the freestream flow and general fluid behavior within the domain. Figure 5 contains geometrical properties pertaining to Case 2, and Figure 6 contains the two-dimensional fence cross sections of Cases 2, 3 and 4.

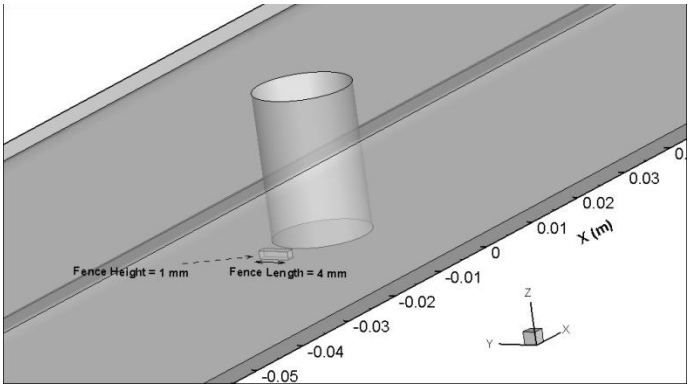

Figure 5. The fence used in Case 2

In this study we preferred to use a two-equation turbulence model since such models provide a fine compromise between accuracy and fast computing. Due to its reputation for working well with flows having a strong adverse pressure gradient, the k- ω model with Shear Stress Transport (SST) was chosen for this study. The solver used for computations was FLUENT's pressure based, implicit solver. The computations were run under steady conditions. The solution scheme used second order discretizations for all the variables in the solution equations. The pressure-velocity coupling was set to the "coupled" mode.

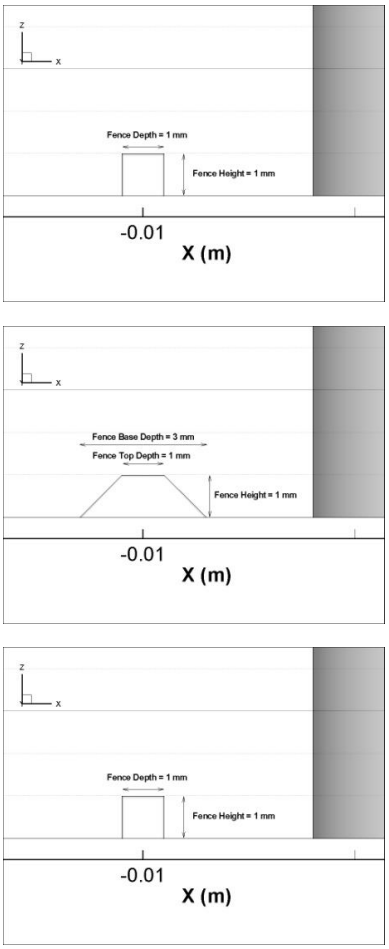

Figure 6. Cross sections of the fences

The inlet velocity profile of the current study was derived from the extensive measurements made by Zaccaria [23] in his studies, and it contained a boundary layer. Calculation of the Reynolds number of the computations was based on the cylinder diameter and found equal to 11000. Flow was assumed to be fully turbulent and incompressible, since this would best represent the fluid flow within the turbine just downstream of the combustor.

The turbulence criteria were the turbulence intensity and turbulence length scale; the turbulence intensity was set to 1% and the turbulence length scale was set to the maximum possible eddy length, which was the cylinder height of 18 mm. Standard values were selected for the inlet static pressure, air density and viscosity.

In order to ensure that the modeling used for the computations - the meshing conducted in Gambit and subsequent simulations carried out by using Fluent - is correct, it was decided to numerically reproduce the results of a previously published experimental work involving a vertical cylinder in cross flow mounted on a wall. The work in mention was selected to be Eckerle's Ph.D thesis [7].

Eckerle [7] published a significant amount of data in his thesis, including the static pressure coefficient C_{P_S} and the velocity profiles at the inlet of the domain. The reproduction of his domain was carried out using Gambit, then the case was run in Fluent to regenerate the results.

Our results and Eckerle's were compared based on the static pressure coefficient calculated on a cylinder surface line 156 mm above the bottom wall, a line which extends from the 0 degree plane to the 90 degree plane, according to the following formula:

$$C_{P_S} = \frac{P_{S_{Cylinder}} - P_{s_{Inlet}}}{\frac{1}{2}\rho {U_{Inlet}}^2} \qquad (1)$$

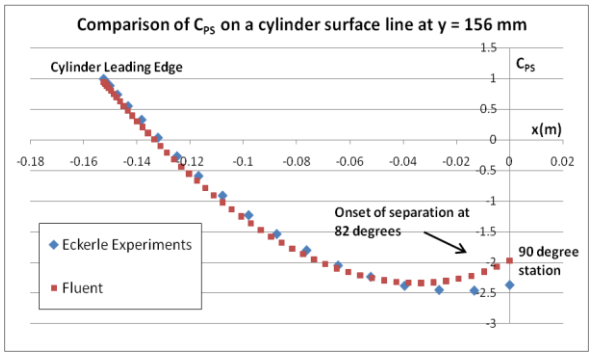

Figure 7. Comparison of C_{P_S} based on a previously published work [7] and on our results

The graph presented in Figure 7 is a strong proof that the modeling used in Fluent will generate results that show good agreement with experimental results, since the agreement between the two curves is 95% in general.

The final step before beginning the simulation of each case was to conduct a grid independence study. The purpose of the grid independence study is to choose the computational mesh with the lowest number of three dimensional cells which gives an accurate representation of the flow conditions within the flow domain. The most effective way, of determining at which point the desired accuracy is obtained, is to relate the grid independence to a crucial flow parameter. One such parameter is the static pressure coefficient calculated over a line on the cylinder surface, according to Equation 1.

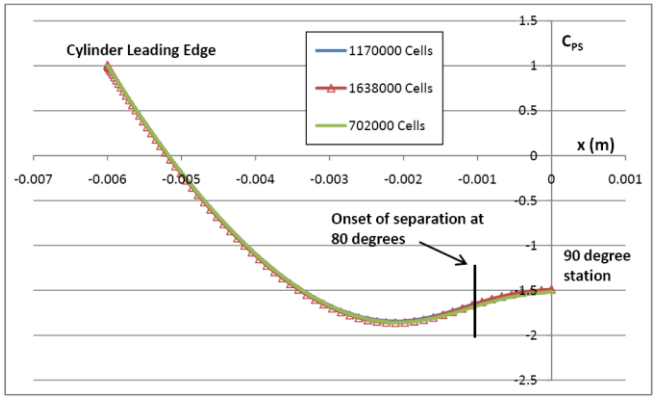

Figure 8. Comparison of C_{P_S} for the baseline case computed with three different mesh sizes

Figure 8 depicts the C_{P_S} curves for cases conducted with three different mesh sizes: The curves are almost identical, thus the mesh having the second lowest number of cells was chosen for the calculation of the baseline case. The lowest mesh size was not selected, because it was thought that the mesh sizes for the cases involving upstream fences would easily be greater than 1 million, a guess later turned out to be true. Thus, a mesh size of 1170000 was selected for the baseline case in order to keep the order of magnitude of the mesh sizes for all four cases the same. This study also acted as another validation tool for the accuracy of the results generated by Fluent since the results have been shown to be independent of the grid size.

Please refer to Gokce [24] for further methodology details, verification methods and geometrical information which are not presented here for the sake of brevity.

RESULTS AND DISCUSSION

In the following figures, visualization of the streamlines in the streamwise plane of symmetry (at y = 0) depicts where and how the horseshoe vortex formed in each study case, with each case containing the same number of streamlines, originating from the same rakes with the same density. This was done to conduct a meaningful comparative analysis of the cases.

Figure 9 is a close up view of the streamlines in the plane of symmetry for the baseline case, showing a set of four vortices, in keeping with previously published studies such as the work of Ishii and Honami [25].

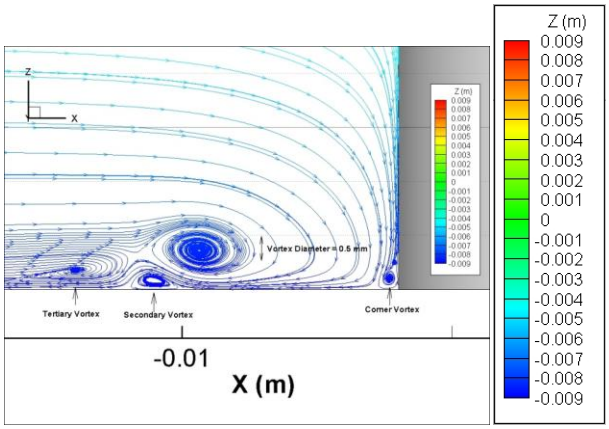

Figure 9. Roll-up of the baseline case

Figure 10 provides an overall look at the streamlines in the plane of symmetry of all of our cases, and shows that all of the fence configurations we used successfully modified the position of the main roll-up, and that the oblique fence resulted in complete removal of secondary vortices.

Figure 11 consists of a graphical representation of the three dimensional streamline analysis of the baseline case, showing the formation of the horseshoe vortex in detail. It reveals that the wake of the cylinder is highly turbulent, where a vortical structure initiated near the hub is transmitted higher towards the top of the cylinder. The legs of the horseshoe vortex experience a rise as they travel away from the cylinder, in agreement with previously published work [5-7].

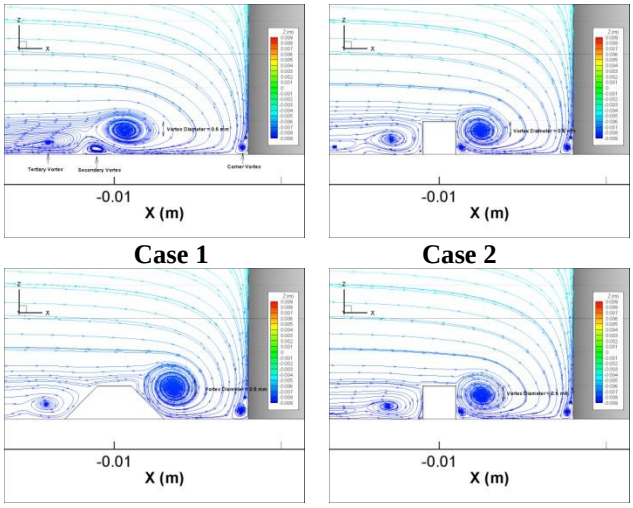

Figure 10. 2D streamlines for all cases **(legend is in Figure 9)**

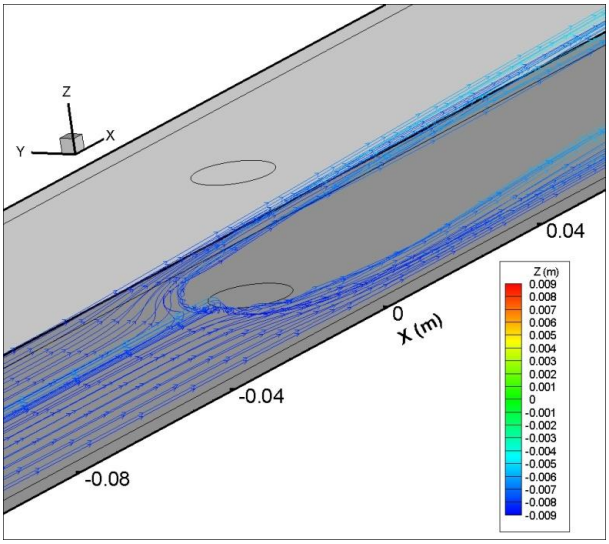

Figure 11. 3D streamlines for the baseline case **(legend is in Figure 9)**

Figure 12 displays the three-dimensional streamlines upstream of the cylinder leading edge for all cases to enable comparison. Comparative detailed assessment of close up views of the three dimensional streamlines within the wakes of each case (figures not shown) revealed that when a fence was added, the streamlines were modified in the turbulent wake, rising less in general before moving downstream.

The variation of total pressure (gauge) and velocity magnitude along vertical (y-z) planes spaced 3 mm apart are displayed for the baseline case in Figure 13 and show the total pressure drop within the cylinder wake expected for a cylinder in viscous flow according to prior descriptions [26-28].

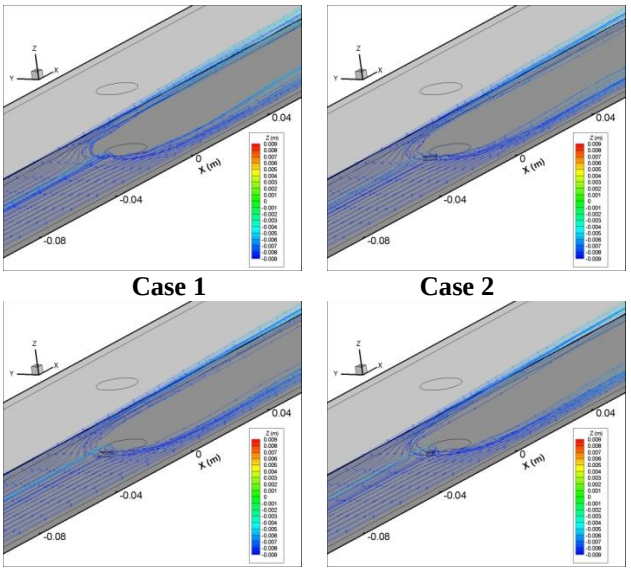

Figure 12. 3D streamlines for all cases **(legend is in Figure 9)**

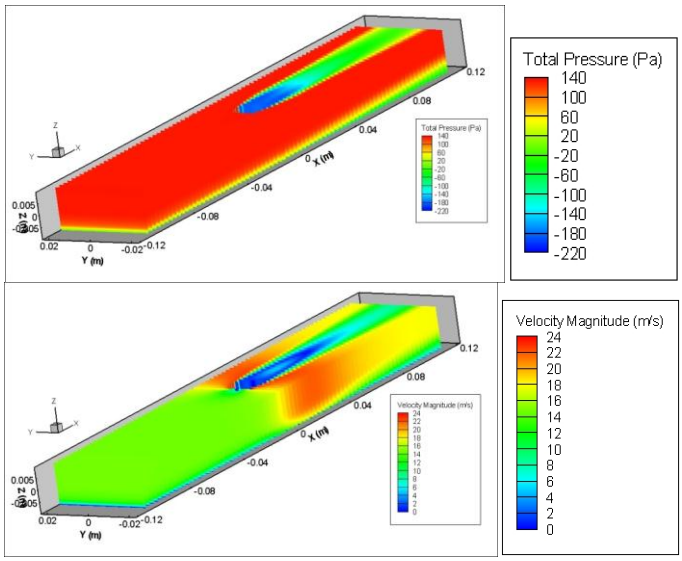

Figure 13. Total pressure and velocity magnitude contours along the entire domain

The legends for Figure 14 through 19 are located in Figure 13.

Initially, the flow moving over the cylinder accelerated from the 0 degree plane (the streamwise plane of symmetry) to the 80 degree plane. Then, the adverse pressure gradient began to decelerate the flow and the flow separated from the cylinder, resulting in a low velocity within the wake. The total pressure and velocity magnitude contours for Case 2, 3 and 4 were similar to the baseline case, as can be ascertained from Figures 14 and 15, demonstrating that the effects of placing a fence upstream of the cylinder were not carried into the freestream and that the general behavior of the flow was not changed. This is a favorable feature since we did not wish to change the main attributes of the flow.

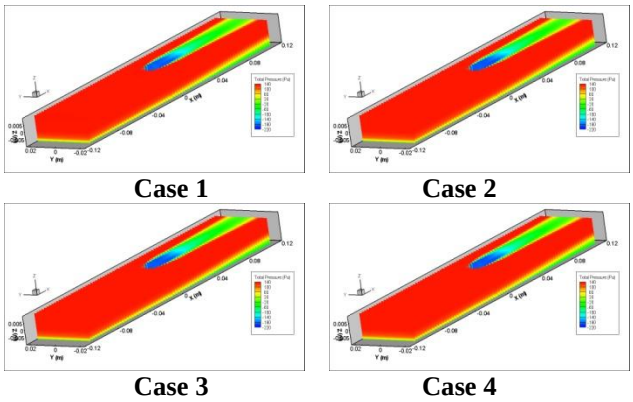

Figure 14. Total pressure variation for all cases

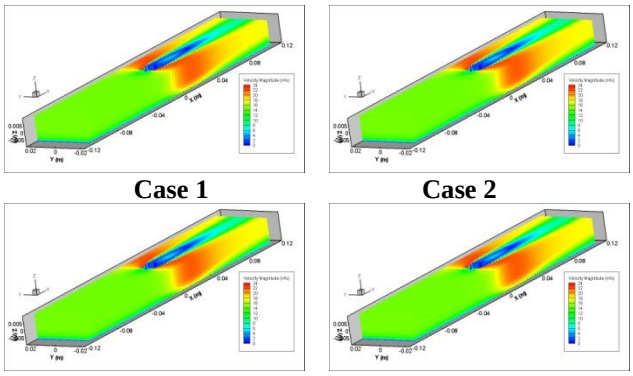

Figure 15. Velocity magnitude variation for all cases

In this study, the variation of total pressure and velocity magnitude contours near the streamwise position where the endwall shape modification was located was of specific interest, as it would clarify the initiation of the vortex and its extension downstream. Figures 16(a), (b) and (c) show total pressure contours at x = -0.01, x = -0.009 and x = -0.006 for the baseline case at the location of the initial roll-up, at slightly downstream of the initial roll-up and at the cylinder leading edge, respectively. The small elliptical region located at y = 0 within 1 mm of the endwall in Figures 16(a) and (b) are the projections of the initial roll-up onto the y-z plane; the vortical regions where the total pressure is low in Figure 16(c) are the projections of the horseshoe vortex onto the y-z plane.

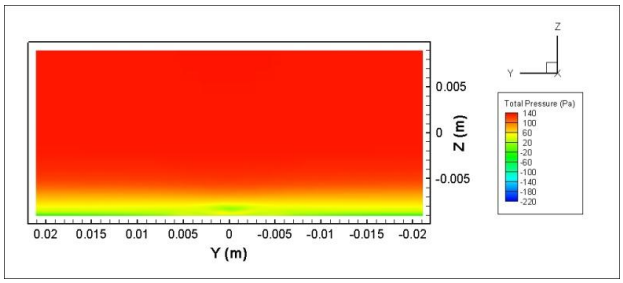

Figure 16(a). Initial roll-up location

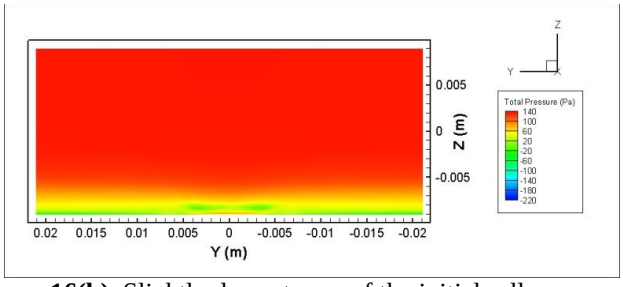

Figure 16(b). Slightly downstream of the initial roll-up location

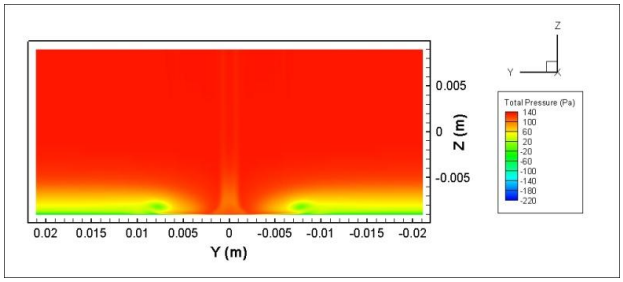

Figure 16(c). At the cylinder leading edge

Figure 17 allows comparison of total pressure contours on a y-z plane located at x = -0.006, i.e. the cylinder leading edge for all cases, showing that rectangular fences decreased the distance between the vortex legs by 19%, whereas the oblique fence decreased it by 31% compared to the baseline case, upstream of the cylinder leading edge.

The three-dimensional analysis of the streamlines in our study suggested that there might be a difference in the velocity magnitudes within the turbulent cylinder wake, because the streamlines appeared to rise to different heights based on the type of fence used. Velocity magnitude analysis at three y-z cross sections along the x-axis downstream of the cylinder were used to clarify this situation. Figures 18(a), (b), (c) show velocity magnitude contours at x = 0.009, x = 0.012 and at x = 0.015, at 3 mm, 6 mm and 9 mm downstream of the cylinder trailing edge, respectively, for the baseline case, and display the path of the legs of the horseshoe vortex, as well as the low velocity region within the wake.

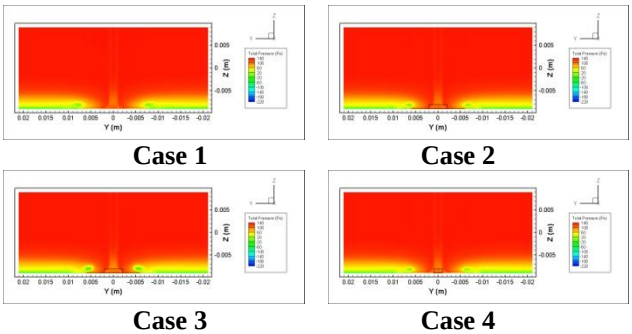

Figure 17. Comparison of total pressure distributions at the cylinder leading edge

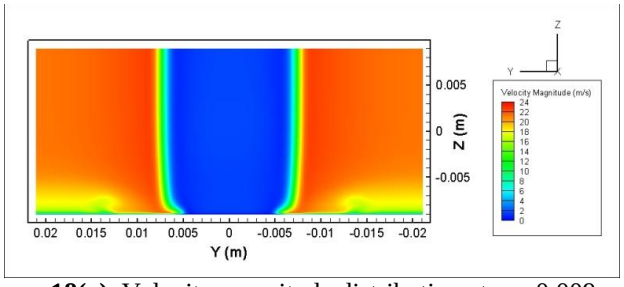

Figure 18(a). Velocity magnitude distribution at x = 0.009 m

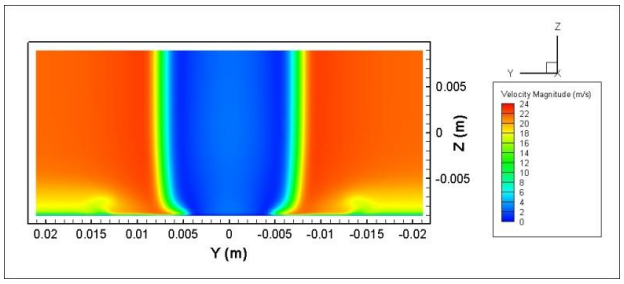

Figure 18(b). Velocity magnitude distribution at x = 0.012 m

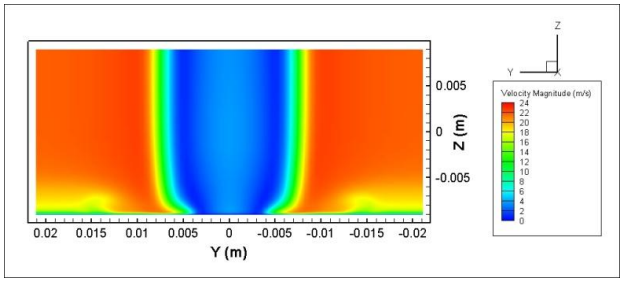

Figure 18(c). Velocity magnitude distribution at x = 0.015 m

Analysis of velocity magnitude contours obtained for the other cases at the same locations revealed that the addition of a non-oblique fence in Case 2 and 4 caused a 7%, whereas the oblique fence added in Case 3 caused a 14% decrease in the distance between the legs of the horseshoe vortex downstream of the cylinder; this vortex-contracting effect is shown in Figure 19 which depicts the velocity magnitude of all cases on a y-z plane located at x = 0.018 m, 12 mm (one cylinder diameter) downstream of the cylinder trailing edge.

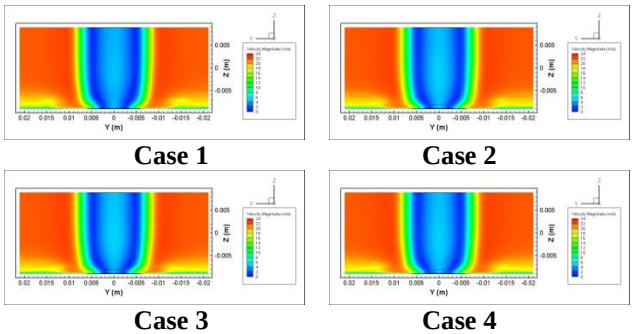

Figure 19. Comparison of velocity magnitude contours at x = 0.018 mm

In our study, the wall shear stress contours on the endwall and cylinder surfaces provided another useful perspective of flow behavior within the simulated domains. Figures 20(a) and (b) depict wall shear stress over the hub and cylinder surfaces for the baseline case in three and two dimensional form, respectively, and demonstrate the symmetric nature of the horseshoe vortex.

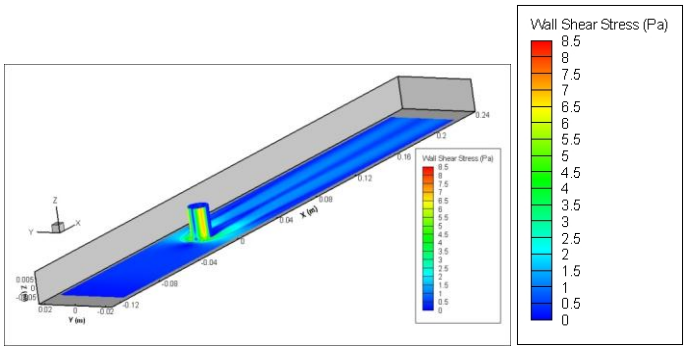

Figure 20(a). Wall shear stress over the baseline case's domain

It is evident that the pattern of the horseshoe vortex is made visible by an increased wall shear stress value compared to the values just upstream of the horseshoe vortex, with the wall shear stress over the region lying between the cylinder and the vortex being higher than the rest of the values over the entire hub, except for the small strips over the cylinder surface.

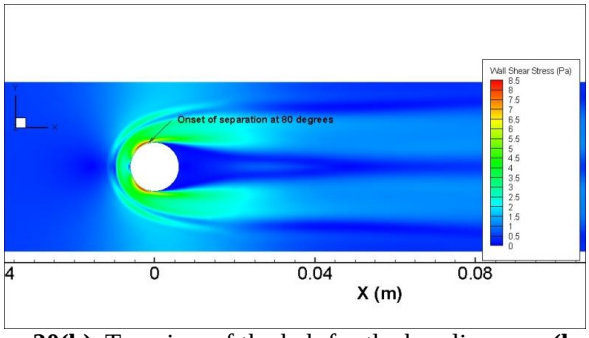

Figure 20(b). Top view of the hub for the baseline case **(legend is in Figure 20a)**

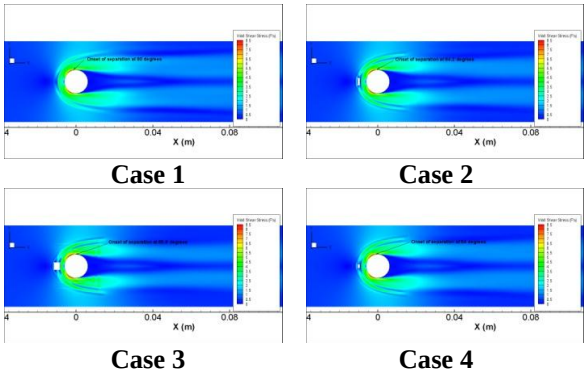

Figure 21. Comparison of the hub shear stress distribution for all cases **(legend is in Figure 20a)**

Demonstrated in Figure 21, the general distribution of wall shear stress on the hub was similar in all cases; however, there was a thin region of increased wall shear stress in front of the fences. In addition, the rectangular fences in Case 2 and 4 delayed the separation of the fluid from the cylinder surface by approximately 4 degrees, whereas the oblique fence in Case 3 delayed it by approximately 6 degrees, compared to the baseline case. The wall shear stress distribution near the oblique fence was different than the non-oblique (rectangular) fence cases. This was also reflected by the different contraction amounts in the lateral distance between the legs of the horseshoe vortex for the two fence types.

One of the main goals of this study was to add upstream endwall fences that could attenuate horseshoe vortex formation in an environment simulating a cylinder subjected to cross flow while achieving nil or minimal effect on freestream flow. Analysis of total pressure and velocity magnitude contours along the streamwise axis presented above indicate that the freestream was not affected by the presence of the fences simulated in this study. The variation of total pressure and velocity magnitude found along horizontal planes placed 0.5, 3, 6 and 9 mm above the hub were assessed as another means of determining whether the effects of placing a fence extended to the freestream or not. Figures 22(a), (b), (c) and (d) show the total pressure contours found in the baseline case, on a horizontal surface (whose normal vector is in the z direction) situated 0.5, 3, 6 and 9 mm above the hub, respectively.

The legends for Figure 22(a) through 27 are located in Figure 13.

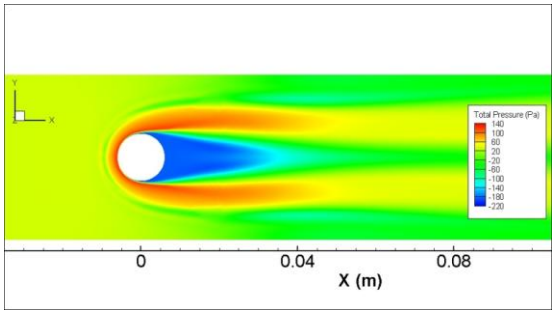

Figure 22(a). Total pressure variation 0.5 mm above the hub; baseline case

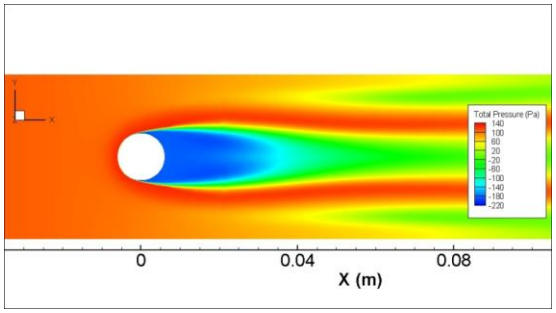

Figure 22(b). Total pressure variation 3 mm above the hub; baseline case

When the horizontal contours of total pressure of all cases were compared in Figures 23 and 24, it was observed that the addition of a fence created changes in total pressure near the hub but it did not affect the freestream values, signifying that the fence configurations used in this study were capable of avoiding an alteration in the freestream properties of the flow.

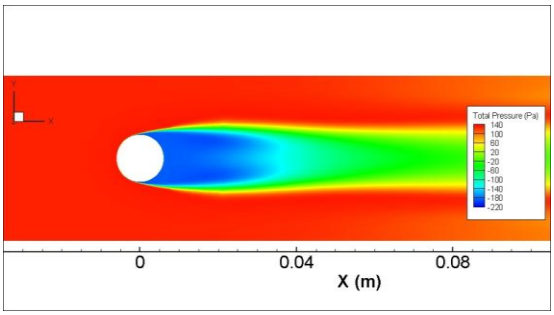

Figure 22(c). Total pressure variation 6 mm above the hub; baseline case

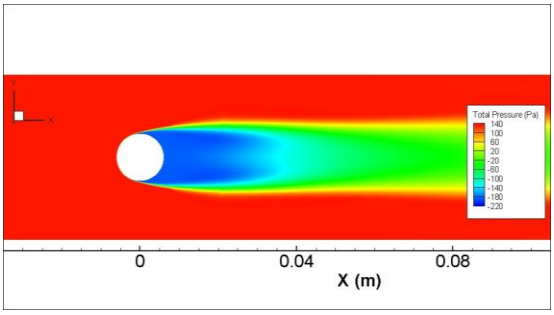

Figure 22(d). Total pressure variation 9 mm above the hub; baseline case

Figures 25(a) through (d) exhibit the velocity magnitude of the baseline case on a horizontal surface situated 0.5, 3, 6 and 9 mm above the hub, respectively; their analysis showed that the flow stagnated near the location of the initial roll-up. This was not present in x-y planes lying above the horseshoe vortex, demonstrating that the horseshoe vortex is limited to the first 2 millimeters as indicated previously by the streamlines in the streamwise plane of symmetry.

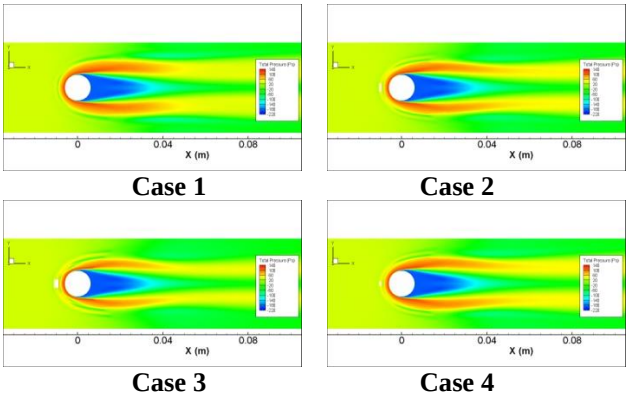

Figure 23. Comparison of total pressure contours 0.5 mm above the hub

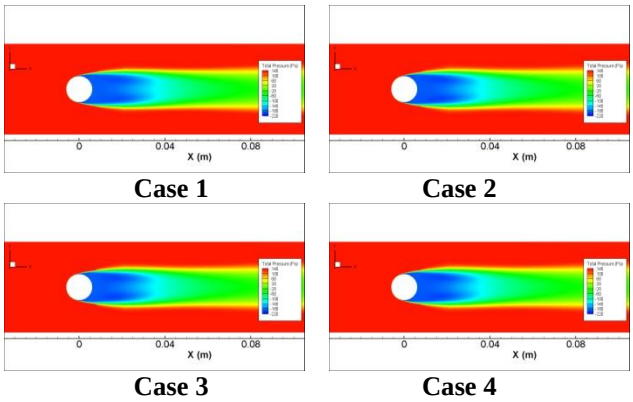

Figure 24. Comparison of total pressure contours 9 mm above the hub

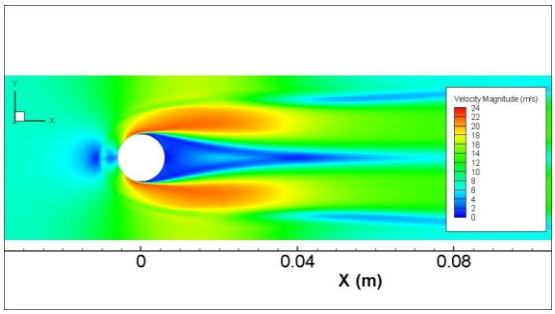

Figure 25(a). Velocity magnitude contours 0.5 mm above the hub

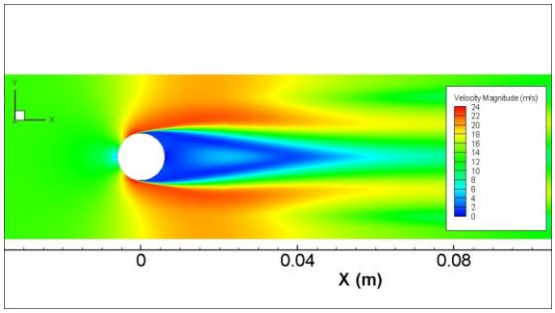

Figure 25(b). Velocity magnitude contours 3 mm above the hub

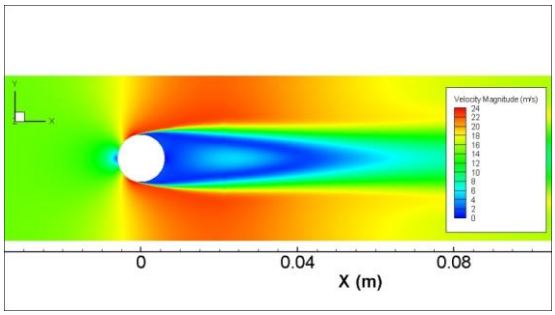

Figure 25(c). Velocity magnitude contours 6 mm above the hub

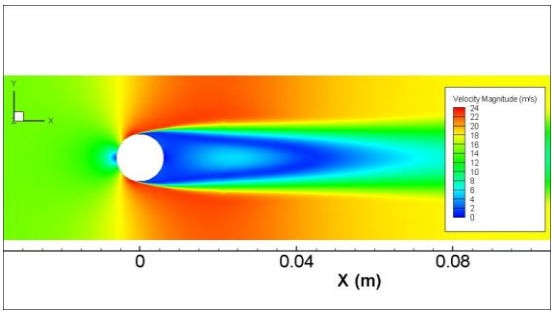

Figure 25(d). Velocity magnitude contours 9 mm above the hub

Figures 26 and 27 consist of graphical presentations of the velocity magnitude distribution of all the cases on a horizontal surface 0.5 and 9 mm above the hub, respectively; comparative assessment revealed that the area of the region where the velocity was very low, located near the main vortex roll-up, decreased by 20% when a fence was added, irrespective of its being oblique or not. This can be explained by the fact that, compared to baseline conditions, the addition of a fence in our simulated environment caused an increase in the roll-up of high-momentum fluid into the low-momentum area near the hub, thereby increasing velocity magnitude near the fence.

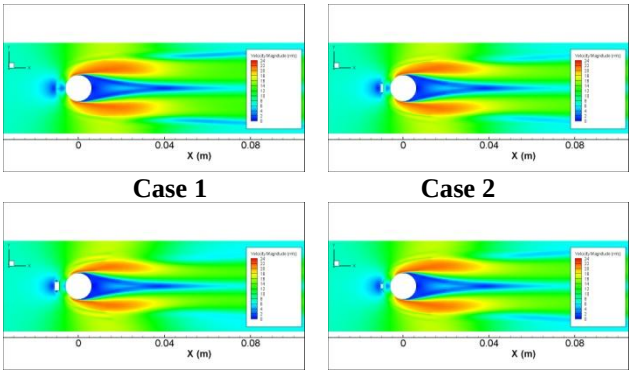

Figure 26. Comparison of the velocity magnitude contours 0.5 mm above the hub for all cases

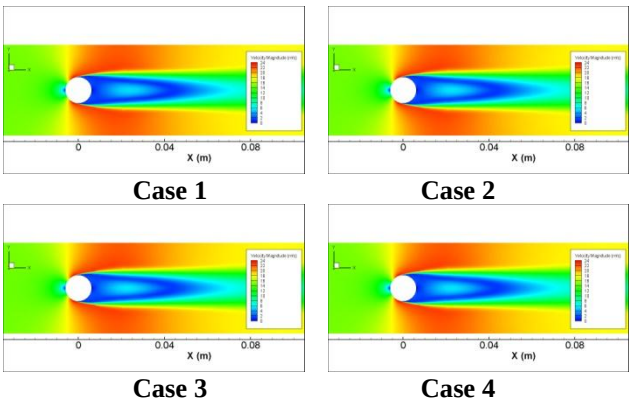

Figure 27. Comparison of the velocity magnitude contours 9 mm above the hub for all cases

As with the total pressure contours, comparing the velocity magnitude contours of our study cases demonstrated that the effects of placing a fence upstream of the cylinder did not extend any further than the first 2 millimeters above the hub endwall surface, thus precluding the risk of extensive and negative flow alterations in the cylinder environment. In other words, the results presented up to this point suggest that the effects of the horseshoe vortex and the fences are limited to the first two millimeters above the hub endwall surface.

Since the presence of the fences could have an effect on the total pressure distribution within the first 2 mm region in mention, the bottom 2 millimeters of y-z planes placed along the streamwise axis were clipped and the C_p values along these thin strips estimated with the equation given below were plotted for each case; they are presented together for comparison in Figure 28.

$$C_P = \frac{(P_0)_{2\ mm\ Strip} - (P_0)_{2\ mm\ Inlet\ Strip}}{\frac{1}{2}\rho(U_{2\ mm\ Inlet\ Strip})^2} \qquad (2)$$

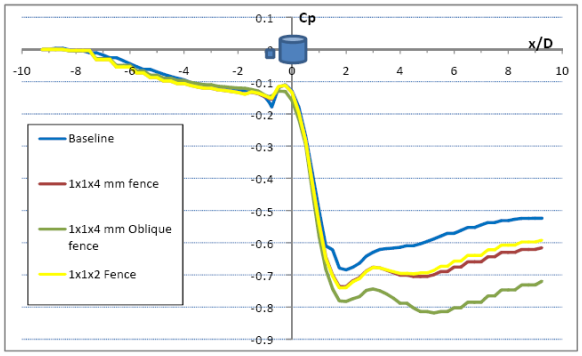

Figure 28. Mass averaged total pressure based Cp curves

The total pressure and velocity magnitude values used in the equation above were mass-averaged values. The locations of the cylinder and fence are represented by the blue colored geometric shapes in Figure 28, which depicts similar C_p curves for all cases. However, when the region between two specific locations, one slightly upstream of the fence location at x/D = -1 and the other one at the cylinder leading edge at x/D = -0.5, was inspected closely, cases employing fences showed an increase in mass averaged total pressure when compared to the baseline case, in that region. This is demonstrated in Figure 29, comprising a close-up view of the C_p gains of the cases, where the blue colored curve belongs to the baseline case, and the others represent the cases with fences.

The curves for the cases employing a fence all had higher values than the baseline case within the region of interest defined above, located in the vicinity of the fence, where gain ranged from 1.3% at its lowest value to 13.9% at its highest. Thus, it was concluded that the presence of a fence created a positive change in mass averaged total pressure levels near the hub-fence junction, compared to the baseline case. Although all fence cases showed a slight increase in mass averaged total pressure loss far downstream of the cylinder, this latter effect

did not appear as a significant complication in the light of the C_p gain achieved upstream with the addition of a fence.

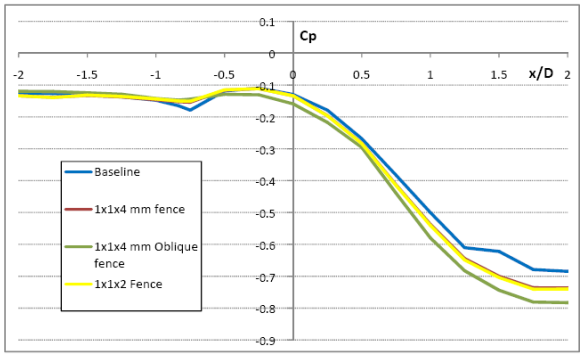

Figure 29. Close-up view of Figure 28

CONCLUSIONS AND RECOMMENDATIONS

In this article, the flow properties and streamline patterns for three different configurations of an endwall fence placed upstream of a vertical cylinder in cross flow are presented, along with the results for the baseline case consisting of a cylinder only. The flow for the four cases in mention was simulated using the commercially available Fluent software (version 6.3) developed by ANSYS.

The main purpose of this study was to investigate the effects of placing an endwall fence upstream of a cylinder in cross flow using numerical computations, with the expectation of obtaining improvements in flow behavior without causing any changes to the freestream. To this end, a baseline case with no fence was compared with three other cases having varying fence configurations. The numerical modeling strategy, i.e. the computerized simulation approach used in the current study produced results that were in accordance with previously published experimental data [7] for a simple cylinder in cross flow only. Thus, the accuracy of our method and the potential applicability of our findings to real life turbine systems were validated.

Our results can be summarized as follows:

1) The streamline patterns produced in the streamwise plane of symmetry for the baseline case agreed very well with previously published studies. A clearly visible main horseshoe vortex formed upstream of the cylinder; a secondary vortex and a tertiary vortex were situated slightly upstream of the main vortex. A corner vortex of relatively smaller scale formed at the cylinder-endwall junction.

2) The 1 x 1 x 4 mm and the 1 x 1 x 2 mm fences decreased the lateral distance between the two legs of the horseshoe vortex by 19% upstream and by 7% downstream of the cylinder.

3) The 1 x 1 x 4 mm oblique fence decreased the lateral distance between the two legs of the horseshoe vortex by 31% upstream and by 14% downstream of the cylinder.

4) The 1 x 1 x 4 mm and 1 x 1 x 2 mm fences caused the x-coordinate of the main vortex center to move by 13% downstream.

5) The 1 x 1 x 4 oblique fence moved the x-coordinate of the main vortex center by 18% downstream and its z-coordinate by 20% upwards.

6) The shifting of the x-coordinate and z-coordinate of the center of the main vortex roll-up observed in the presence of fences indicated that adding endwall fences upstream of a cylinder in cross flow could help control and modify associated horseshoe vortex formation.

7) The effects of using a 1 x 1 x 4 mm and 1 x 1 x 2 mm non-oblique fence seemed almost identical. Hence, the positive effects generated by the fence seemed to be influenced by the height of the fence rather than its length. Therefore, it appears possible to use a shorter fence to generate improvements in flow behavior.

8) The oblique fence prevented the formation of secondary vortices both in front of and behind the fence.

9) Although a slight increase in mass averaged total pressure loss was found far downstream of the cylinder in an environment containing a fence, improvements in mass averaged total pressure gain ranging from 1.3% to 13.9% near the fence, within strips covering the first 2 mm above the hub were also observed.

10) The improvements described occurred without altering the freestream.

When considered together, our results suggest that adding an endwall fence upstream of a cylinder subjected to cross flow improves flow characteristics mainly by attenuating horseshoe vortex formation. These findings could have important practical implications. Since the cylinder in our simulated system served as a representative of a turbine nozzle guide vane (NGV) blade, the improved flow attributes we observed with the addition of a fence suggest the possibility of a similar effect in an actual turbine environment, where smoother and more predictable flow behavior in the turbine passage could be expected, if the interaction of horseshoe vortices produced by consecutive blades in a row of NGV blades could potentially be decreased in the presence of upstream fences. If such an effect could be proved under experimental conditions, it could serve as an important starting point for developing a practical method of increasing turbine efficiency.

The positive changes in flow attributes created by the presence of fences of varying shapes indicate that this type of modification is a promising candidate to modify the aerodynamic characteristics of real life turbines. The results of this work show that this topic warrants detailed wind tunnel tests and other experiments to further understand the effects of using endwall fences to reduce the detrimental effects of horseshoe vortices in different flow environments. Such investigations could have relevance not only for aerospace engineering, but for other scientific fields as well.

REFERENCE

1. Sieverding, C. H., 1985, *Recent Progress in the Understanding of Basic Aspects of Secondary Flows in Turbine Blade Passages*, ASME Journal of

Engineering for Gas Turbines and Power, Vol. 107, pp.248-257
2. Mattingly, J. D., *Elements of Propulsion: Gas Turbines and Rockets*, 2nd ed., 2006, American Institute of Aeronautics and Astronautics, Reston, Virginia
3. Hill, P. G. and Peterson, C. R., Mechanics and Thermodynamics of Propulsion, 2nd ed., 1992, Addison-Wesley, Reading, Massachusetts
4. Langston, L. S., Nice, M. L., and Hooper, R. M., 1976, *Three-Dimensional Flow Within a Turbine Cascade Passage*, ASME Paper No. 76-GT-50.
5. Eckerle, W. A. and Awad, J. K. 1991, *Effect of Freestream Velocity on the Three-Dimensional Separated Flow Region in Front of a Cylinder*, ASME Jour. of Fluids Engineering. Vol. 113, pp. 37-44
6. Eckerle, W. A. and Langston, L. S. 1987, *Horseshoe Vortex Formation Around a Cylinder*, ASME Jour. Of Turbomachinery. Vol. 109, pp. 278-285.
7. Eckerle, W.A., *Horseshoe Vortex Formation Around a Cylinder*, Ph.D Thesis, University of Connecticut, Storrs, CT, May 1985
8. Praisner, T. J. and Smith, C. R. 2006, *The Dynamics of the Horseshoe Vortex and Associated Endwall Heat Transfer-Part I: Temporal Behavior*, Journal of Turbomachinery. Vol. 128, No.4, pp. 747-754
9. Praisner, T. J. and Smith, C. R. 2006, *The Dynamics of the Horseshoe Vortex and Associated Endwall Heat Transfer-Part II: Time Mean Results*, Journal of Turbomachinery. Vol. 128, No.4, pp. 755-762
10. Hada, S., Takeishi, K., Oda, Y., Mori, S., and Nuta,Y. 2008, *The Effect of Leading Edge Diameter on the Horse Shoe Vortex and Endwall Heat Transfer*, Proceedings of the ASME Turbo Expo, Vol 4, Part A, pp. 813-823
11. Goldstein, R.J. and Karni, J. 1984, *The Effect of a Wall Boundary Layer on Local Mass Transfer From a Cylinder in Crossflow*, Transactions of the ASME. Journal of Heat Transfer. Vol. 106, No. 2, pp. 260-267
12. Visbal, M. R., 1991, *Structure of Laminar Juncture Flows*, AIAA Journal, Vol. 29, pp.1273-1282
13. Kang, K. J., Kim, T. and Song, S. J., 2009, *Strengths of Horseshoe Vortices around a Circular Cylinder with an Upstream Cavity*, Journal of Mechanical Science and Technology, Vol. 22, pp. 1773-1778
14. Camci, C. and Rizzo, D. H., 2002, *Secondary Flow and Forced Convection Heat Transfer Near Endwall Boundary Layer Fences in a 90^o Turning Duct*, International Journal of Heat and Mass Transfer, Vol 45, No. 4, pp. 831-843
15. Rizzo, D. H., *The Aerodynamic and Heat Transfer Effects of an Endwall Boundary Layer Fence in a 90^o Turning Square Duct*, M.S Thesis, The Pennsylvania State University, State College, PA, May 1994
16. Prümper, H., 1972, *Application of Boundary Fences in Turbomachinery*, AGARD AG No. 164. Paper No. II-3: 315-331
17. Turgut, H. O., 2007-Present, Private Communications, The Pennsylvania State University
18. Kirkil, G., Constantinescu, S. G., Ettema, R. 2008, *Coherent Structures in the Flow Field around a Circular Cylinder with Scour Hole*, Journal of Hydraulic Engineering, Vol. 134, No. 5, pp. 572-587
19. Gokce, Z. O. and Camci, C., 2011, *Unsteady Flow Characteristics and Viscous Flow Losses Behind Multiple Rows of Circular Pin Fins in Coolant Channels*, ASME 2011 International Mechanical Engineering Congress and Exposition, ASME/IMECE2011-64333, November 11-17 2011, Denver, Colorado, In Publication
20. Kavurmacioglu, L., Dey, D. and Camci, C. July 2007, *Aerodynamic Character of Partial Squealer Tip Arrangements in an Axial Flow Turbine, Part I: Detailed Aerodynamic Field Modifications via Three Dimensional Viscous Flow Simulations Around Baseline Tip*, Progress in Computational Fluid Dynamics, Vol. 7, pp. 363-373
21. Kavurmacioglu, L., Dey, D. and Camci, C. July 2007, *Aerodynamic Character of Partial Squealer Tip Arrangements in an Axial Flow Turbine, Part II: Detailed Numerical Aerodynamic Field Visualizations via Three Dimensional Viscous Flow Simulations Around a Partial Squealer Tip*, Progress in Computational Fluid Dynamics, Vol. 7, pp. 374-386
22. Rao, N., Kavurmacioglu, L., Gumusel, B. and Camci, C., 2006, *Influence of Casing Roughness on the Aerodynamic Structure of Tip Vortices in an Axial Flow Turbine*, ASME Paper GT2006-91011, presented at the ASME International Gas Turbine Congress in Barcelona, Spain.
23. Zaccaria, M. A., *An Experimental Investigation into the Steady and Unsteady Flow Field in an Axial Flow Turbine*, Ph.D Thesis, The Pennsylvania State University, State College, PA, December 1994.
24. Gokce, Z. O. *Comparative Numerical Analysis of Flow Development in the Presence of Endwall Fences Upstream of a Vertical Cylinder in Cross Flow*. M.S Thesis, The Pennsylvania State University, PA, May 2010.
25. Ishii, J. and Honami, S. 1986, *Three-Dimensional Turbulent Detached Flow with a Horseshoe Vortex. Journal of Engineering for Gas Turbines and Power*, Vol 108., No.1, pp. 125-130
26. White, F. M., *Fluid Mechanics*, 6th ed., 2008, McGraw-Hill, New York, New York
27. Wilcox, D. C., *Basic Fluid Mechanics*, 3rd ed., 2007, Birmingham Press, Inc., San Diego, California
28. Anderson, J. D., Jr., *Fundamentals of Aerodynamics*, 3rd ed., 2001, McGraw-Hill, Boston, Massachusetts